



## SYMPOSIUM

### The Role of Water in Fast Plant Movements

J. Edwards,<sup>1,\*</sup> M. Laskowski,<sup>†</sup> T. I. Baskin,<sup>‡</sup> N. Mitchell,<sup>§</sup> and B. DeMeo<sup>¶</sup>

\*Department of Biology, Williams College, Williamstown, MA 01267, USA; <sup>†</sup>Department of Biology, Oberlin College, Oberlin, OH 44074, USA; <sup>‡</sup>Department of Biology, University of Massachusetts, Amherst, MA 01003, USA; <sup>§</sup>Department of Biology, University of New Mexico, Albuquerque, NM 87131, USA; <sup>¶</sup>Department of Biomedical Informatics, Harvard Medical School, Boston, MA 02115, USA

From the symposium “Playing with Power: Mechanisms of Energy Flow in Organismal Movement” presented at the annual meeting of the Society for Integrative and Comparative Biology, January 3–7, 2019 at Tampa, Florida.

<sup>1</sup>E-mail: jedwards@williams.edu

**Synopsis** Plants moved onto land ~450 million years ago and faced their biggest challenge: living in a dry environment. Over the millennia plants have become masters of regulating water flow and the toolkit they have developed has been co-opted to effect rapid movements. Since plants are rooted, these fast movements are used to disperse reproductive propagules including spores, pollen, and seeds. We compare five plants to demonstrate three ways, used alone or in combination, that water powers rapid movements: the direct capture of the kinetic energy of a falling raindrop propels gemmae from the splash cups of the liverwort, *Marchantia*; the loss of water powers the explosive dispersal of the spores of *Sphagnum* moss; the alternate loss and gain of water in the bilayer of the elaters of *Equisetum* drive the walk, jump, and glide of spores; the gain of water in the inner layer of the arils of *Oxalis* drive the eversion of the aril that jettisons seeds from the capsule; and the buildup of turgor pressure in the petals and stamens of bunchberry dogwood (*Cornus canadensis*) explosively propels pollen. Each method is accompanied by morphological features, which facilitate water movement as a power source. The urn shaped splash cups of *Marchantia* allow dispersal of gemmae by multiple splashes. The air gun design of *Sphagnum* capsules results in a symmetrical impulse creating a vortex ring of spores. The elaters of *Equisetum* can unfurl while they are dropping from the plant, so that they capture updrafts and glide to new sites. The arils of *Oxalis* are designed like miniature toy “poppers.” Finally, in bunchberry, the softening of stamen filament tissue where it attaches to the anther allows them to function as miniature hinged catapults or trebuchets.

#### Introduction

The first land plants, liverworts and mosses, arose ~450 million years ago (Qiu et al. 1998; Qiu 2008; Lenton et al. 2012). The most challenging obstacle to life on land was living in a dry environment. Living in air rather than in water meant that plants evolved tools to maintain internal hydration (Yeats and Rose 2013). Over the millennia plants have become masters of regulating water flow. Adaptations to life on land include a waxy cuticle, which provides a barrier to water loss and also can screen out ultraviolet radiation; stomates, which regulate gas exchange including water loss; a vascular system with xylem and phloem tissues; cell walls which surround the plasma membrane and provide mechanical support; and resistant spores, pollen, and seeds. In this paper we use five species to exemplify how plants have

co-opted their water-regulatory tool kit to engineer plant movements that are surprisingly fast. Rapid movements are shaped by natural selection and relate to adaptation and function in a dry environment particularly with respect to enhancing dispersal and genetic mixing. We cover two bryophytes (*Marchantia polymorpha* and *Sphagnum affine*), one monilophyte (*Equisetum arvense*), and two angiosperms (*Cornus canadensis* and *Oxalis corniculata*).

These five species demonstrate a diversity of mechanisms where plants use water to power rapid movements. Plants can use water in three basic ways to move rapidly. They can directly capture the kinetic energy in a falling raindrop (Brodie 1951; Nakanishi 2002). Based on water loss, they can build up elastic energy through compression or tension. Finally, based on water gain they can increase turgor

pressure and build up stored elastic energy (Dumais and Forterre 2012; Forterre 2013). In systems where water is gained or lost, tissues store elastic energy; eventually, rapid movement results when that stored energy is suddenly released. Energy can be released by the tearing of tissue (e.g., in the inner membrane of the moss capsule or the petals of *C. canadensis*), essentially the removal of a “latch” that restricts energy release (e.g., in the stamens of *C. canadensis*). In the case of bilayer systems where one layer swells or shrinks in response to water and the other layer remains relatively stiff, there can be a rapid shift from one conformation to another (e.g., *Equisetum* or *Oxalis*). Here we describe examples where each method is used alone or in combination to power rapid movement.

One function that has repeatedly evolved is the use of rapid movements to propel the transport of spores and seeds. Since most plants are rooted they face the challenge of spreading offspring to new locations. Here we describe how water powers rapid movements, which transport the asexual reproductive propagules of a liverwort, the spores of a moss, the spores of a horsetail, the pollen of a flowering shrub, and the seeds of a perennial flowering herb.

## Study plants

*Marchantia polymorpha*. Splash cups were collected from the liverwort, *M. polymorpha*, which grows abundantly near the base of buildings on the Williams College campus, Williamstown, MA, USA. Although the liverwort is evergreen, gemmae cup production is highest during the growing season. We collected and filmed droplets falling on gemmae cups.

*Sphagnum affine*. We collected capsules of the moss, *S. affine*, from Adams Bog, a classic kettle hole acid bog in Pownal, VT, USA. Capsules are produced primarily in July. In this paper we present data from *S. affine*, a common species in this bog. Moss shoots with developing capsules were collected in small plastic cups filled with bog water. They were kept for up to a week in a refrigerated incubator until they appeared ready to release spores, typically indicated by cavitation on one side of the capsule.

*Equisetum arvense*. We collected fertile shoots of the horsetail, *E. arvense* from gravelly areas along the Green River, close to its confluence with the Hoosic River in late April and early May in Williamstown, MA, USA (42°42'32.8"N 73°11'47.8"W). Reproductive shoots with closed strobili were collected in water filled jars. We kept them in the lab

for 2–3 days until the sporangiophores began to elongate and sporangia were clearly visible and ready for filming.

*Cornus canadensis*. We collected inflorescences with flowers in bud of the bunchberry dogwood, *C. canadensis* during June on Edwards Island, Isle Royale National Park, MI, USA. Flowering stems were placed in water-filled flower picks and transported back to Williamstown, MA, USA, where they were filmed or mailed overnight to Oberlin, OH, USA, for the turgor pressure and pectin studies.

*Oxalis corniculata*. We collected capsules of *O. corniculata*, creeping wood sorrel, a species that grows as self-propagating weeds in the Williams College greenhouse. These small yellow-flowered oxalis are facultatively self-pollinating (Lovett Doust et al. 1985) and are produced year round. Capsules that looked ready to disperse seeds were collected the day they were filmed. In some cases, we triggered seed release by pinching the base of the capsule with tweezers, but in most cases if we waited, seeds would be propelled from the capsules without triggering.

## Materials and methods

High-speed videos of splash dispersal of gemmae from *M. polymorpha*, *E. arvense* spore flight, *C. canadensis* flower opening, and seed dispersal by *O. corniculata* were filmed with one of two high-speed cameras. Color videos were filmed with a Redlake Motion Xtra HG-XR high-speed video camera (Del Imaging Systems, Cheshire, CT, USA) and monochrome videos were filmed with a Phantom v310 video camera (Vision Research, Wayne, NJ, USA). When necessary we augmented lighting with regular incandescent lights, 250 W photo lamps mounted on flexible arms or fiber optic illuminators (Sölarc model: LB50).

To film water droplets splashing gemmae from the cups of *Marchantia*, we used a glass pipette mounted on a standard lab stand. The fall distance was 0.5 m. The droplet size in [Supplementary Video S1](#) and [Fig. 2](#) is 3.54 mm in diameter. We calculated the potential energy of the droplet using the equation for gravitational potential energy,  $GPE = mgh$ , where  $m$  is the mass in kilograms,  $g$  is the acceleration due to gravity ( $9.8 \text{ m/s}^2$ ), and  $h$  is the height above the ground in meters.

Real time video (30 fps) of horsetail spores were filmed using a Cannon EOS Rebel T31 (Tokyo, Japan) or a Sony Handycam DCR-VX2100 (Tokyo, Japan) both attached to a Zeiss Stemi 2000-C dissecting microscope (Oberkochen, Germany). We

triggered spore movement by breathing gently on the spores on a flat plastic disc. The moisture in breath was sufficient to trigger movement of the spores. To film high-speed images of *E. arvense* spores falling from fertile shoots and the dispersal of gemmae from splash cups of *M. polymorpha*, we used the Phantom v310 camera attached to a Leica S8APO dissecting microscope (Wetzlar, Germany) and filmed at 1000 fps for the horsetail spores and 3000 fps for gemmae dispersal. Sporangioophores of *E. arvense* were gently tapped to trigger release of spores.

To determine cell structure of moss capsules and *Equisetum* spores we took SEM images. To prepare the samples they were fixed in 3% glutaraldehyde in 0.1 M HEPES buffer, rinsed three times in HEPES buffer (pH 7.2), put in 1% osmium tetroxide in deionized water for 1 h, and run through a dehydration series (70%, 80%, 90%, 95%, 100% ethanol  $\times 3$ , each for 8 min). Then they were placed in hexamethyldisilazane for 5 min, removed, air dried, and placed on conductive sticky dots. Samples were sputter coated with gold/palladium and imaged on a Scanning FEI Quanta 400 Environmental Scanning Electron Microscope (Portland, OR, USA).

To determine structure of aril-covered seeds of *O. corniculata* samples we prepared thin sections. Samples were fixed in 3% glutaraldehyde in 0.1 M HEPES buffer for 4 h, rinsed three times in HEPES buffer (pH 7.2), put in 1% osmium tetroxide in deionized water for 1 h, rinsed in distilled water, and run through a dehydration series (70%, 80%, 90%, 95%, 100% ethanol, each for 15 min). This was followed by 15 min in propylene oxide (2 $\times$ ), 75% propylene oxide and 25% Embed 812 on a rotator for 1 h, and a mixture of 50% propylene oxide and 50% Embed on a rotator overnight, and 100% Embed 812 for 4 h uncapped on a rotator. Samples were placed in a silicone mold with Embed 812 and polymerized overnight in a 70°F oven. The sample was then sectioned into 2  $\mu$  sections with a diamond knife on a Reichert-Jung Ultracut E ultramicrotome, placed on a glass slide, and stained with a 1% toluidine blue with 1% sodium borate in water.

To determine the impact of turgor pressure on floral opening in *C. canadensis*, we fully submerged individual flower buds in the indicated concentration of sucrose for 4 h. Buds were then removed from the solution and mechanically triggered to open. The extent of filament opening was determined by measuring the distance by which the anthers separated. The extent of petal opening was assigned into five categories: closed, petals 0° (vertical), petals move 45°, petals move 90° (horizontal), petals move 135°, and petals move 180° (fully reflexed). See

Fig. 7B for the locations of measurements. Nine buds per sucrose treatment group were measured. We calculated the mean distances of separation between anthers and the mean degree of petal opening  $\pm 95\%$  confidence intervals. Loess regressions, which weigh all the data points, were done to fit curves. Statistical analyses were done in R version 3.4.1 within R studio version 1.0.153 (R Core Team 2017; RStudio Team 2017).

To determine the role of tissue softening in shaping the trebuchet stamens of *C. canadensis*, we stained flowers with ruthenium red ( $\sim 0.04\%$  in water) for a few minutes and then observed immediately. We also stained flowers with hydroxylamine hydrochloride–ferric chloride as described in Harris et al. (1994). Briefly, flowers were placed in hydroxylamine hydrochloride solution (7% NaOH, 7% hydroxylamine hydrochloride, 60% ethanol) for 5–10 min, followed by 30 s in a 2:1 mixture of 95% ethanol and concentrated HCl, followed by incubation in a mixture of ferric chloride (10% ferric chloride, 1 mM HCl, 60% ethanol). Finally the whole flowers were washed in 60% ethanol and viewed under a dissecting light microscope.

## Results and discussion

### Direct capture of the energy from a falling raindrop by the liverwort, *M. polymorpha*.

Although raindrop power is currently being examined as a potential source of piezoelectric energy (Guigon et al. 2008a, 2008b; Ilyas and Swinger 2017), plants captured the kinetic energy from raindrops as early as the Late Miocene, which is a minimum age estimate for the evolution of the liverwort *Marchantia* (Villarreal et al. 2016). The kinetic energy in a raindrop varies with mass and velocity. At the upper end of values, a large (6.5 mg) raindrop with a terminal velocity of 9.1 m/s has a calculated kinetic energy of 2.7 mJ (Perera et al. 2014). *Marchantia polymorpha* captures raindrop energy in gemmae cups, which serve as splash cups to propel and disperse gemmae, asexual reproductive propagules (Figs. 1 and 2). The upper portion of the cup is cone-shaped and water droplets hitting a cup off-center splash out laterally swooshing gemmae to new locations (Fig. 2 and Supplementary Video S1). We have observed splashed gemmae as far as about 90 cm from the cup although distances as far as 120 cm have been reported (Equihua 1987). Gemmae are produced at the base of the cup with a few being dislodged with each raindrop and dispersal continues with successive raindrops.

### Water loss drives the explosive capsule dehiscence in the moss *S. affine*.

*Sphagnum affine* disperses spores within a flow of air moving as a vortex ring. Being far less subject to friction than ballistically propelled spores, the vortex ring lifts spores to heights where they can be carried long distances by air currents (Whitaker and Edwards 2010). The energy for producing a vortex ring is generated by a shape change from spherical to cylindrical that results from the epidermal cells losing water, contracting laterally (Fig. 3A, B), and pressurizing the air inside the capsule. The capsules also dehisce along the cap circumference so that the cap is attached to the lower portion of the capsule only by the inner membrane, which serves as a “latch” (Fig. 3C). Once the air pressure in the capsule exceeds the strength of the membrane, the capsule explodes, forcing upward a cylindrically symmetric column of air (containing spores), a flow that develops into a vortex ring, penetrating the stationary air above the capsule and then moving

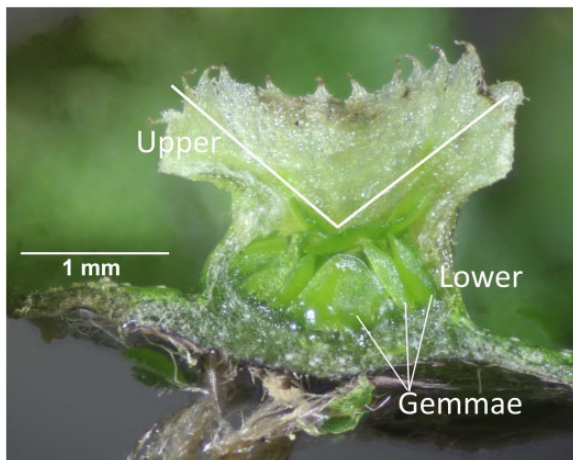


**Fig. 1** Longitudinal section of a *Marchantia polymorpha* gemmae cup shows an upper cone shaped chamber and a lower chamber where gemmae, asexual propagules, are produced.



**Fig. 2** Still frames from a video of a water drop hitting a gemmae cup of *M. polymorpha* off-center and transporting the gemmae-filled droplets. Filmed at 3000 fps with a 20 ms exposure. Arrows point to gemmae in the water droplets. The gravitational potential energy of the falling droplet is  $1.4 \times 10^{-4}$  J. See [Supplementary Video S1](#).

into the turbulent air layer (Fig. 3D and [Supplementary Video S2](#)).

For *S. affine*, our measurements of the timing of capsule transformations indicate that a physiological cue is necessary. Capsules that are dried experimentally do not invariably explode. Whereas if a capsule has begun to transform, typically starting with a cavitation on one side (Fig. 3D), then the transformation from round to cylindrical proceeds rapidly. From the initial cavitation to explosion the capsule undergoes a series of fairly reproducible shape changes over a period of about 21 min (Fig. 3E and [Supplementary Video S3](#)).

### Differential water gain and loss from bilayer of elaters drives the walk, jump, and glide of *E. arvense* spores.

Horsetails (*Equisetum* spp.) are monilophytes (in the fern group) and produce sporangia on distinctive simple cones (strobili) with peltate sporangiophores having hexagonally shaped tops. In mature cones the sporangiophores elongate and the sporangia open releasing green spores, each of which has elaters attached slightly off center forming four arm-like appendages (Fig. 4A). The elaters have a bi-layer structure, with an outer layer that readily absorbs water and an inner layer that is resistant to water uptake (Ueno 1975; Newcombe 1888; Uehara and Kurita 1989). The contents of the outer layer are apparently pectin rich, while the inner layer comprises both cellulose and pectin (see Fig. 4B; Uehara and Kurita 1989).

The movements of *E. arvense* spores are powered by alternate gain and loss of water in the outer layer of the elaters. Water uptake causes the elaters to swell and wrap around the spores (Fig. 4C, frame 1). Drying or water loss causes the elaters to flip out, effecting a jump or walk by the spores (Fig. 4C, frames 2 and 3; [Supplementary Video S4](#)) (Marmottant et al. 2013). The bilayer structure with differential absorption of water defines the

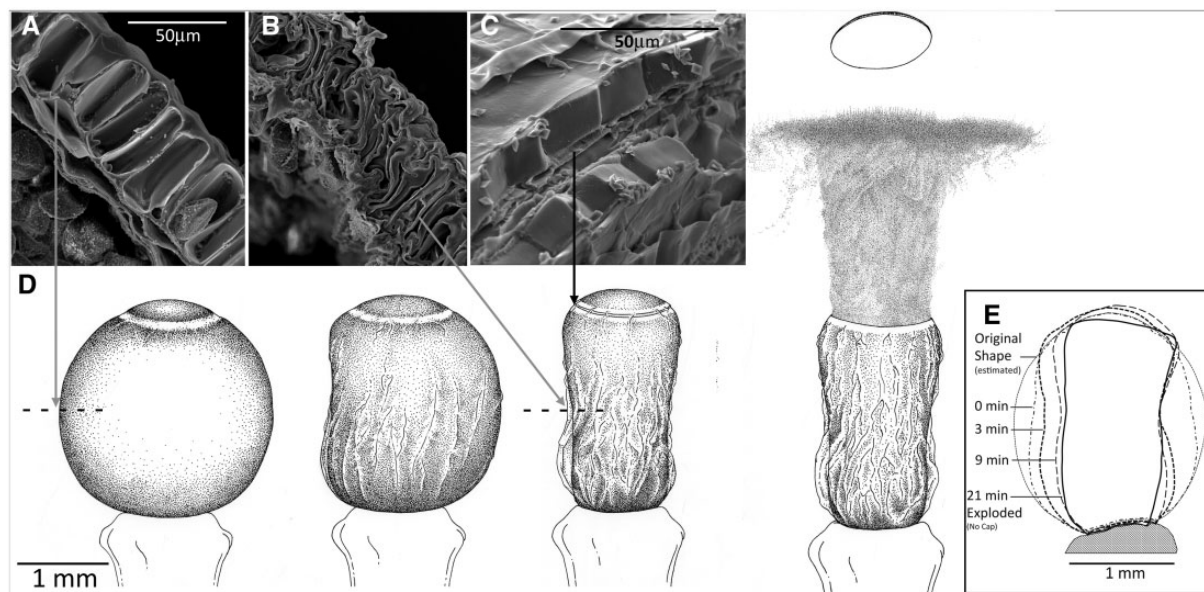


**Fig. 3** The explosive dispersal of *S. affine* spores is powered by water loss (shrinkage) from the capsule cells. **(A)** Cross section of capsule cells when they are fully hydrated. **(B)** Collapsed capsule cells just prior to explosion. Scale is the same as in **A**. **(C)** Detail of the junction between the cap and sides of the capsule showing the inner membrane, which is the “latch” and has to be broken in order for explosive dispersal to occur. **(D)** Four successive stages of capsule shrinkage going from round to columnar and finally the explosion. **(E)** Profiles of a drying capsule showing the rapid shrinkage of the capsule over 21 min. Drawings are to scale from live specimens by Ann Kremers.

shape change with expansion of one layer but not the other creating a curl and storing elastic energy which is released when the elater dries (Marmottant et al. 2013).

We demonstrate that the elaters of horsetail spores are not only used for walking and jumping (Marmottant et al. 2013) but are also used for gliding to new locations. When spores are first released from the sporangia they are still moist and their elaters are curled around the spore. As the moist spores fall, they dry, spread their elaters, and then “catch” the air currents. Their trajectory changes from downward to upward and they can then glide to new locations. Figure 4D with successive stills from a video filmed at 1000 fps shows that when the elaters unfurl, the trajectory tips upward. This allows spores to be dispersed singly and without entanglement with the elaters of other spores (see Supplementary Video S5).

#### The role of water gain in flipping the bilayered arils of *O. corniculata* (creeping wood sorrel).

Typical of the genus, in *O. corniculata* flowers, carpels develop into capsules that extend straight upward when they are mature (Fig. 5A). The capsules split open along five seams and seeds are individually jettisoned from the capsule when the aril surrounding each seed rapidly turns inside out (Figs. 5 and 6,

and Supplementary Video S6). The rapid eversion of the aril is consistent with a bilayer snap-buckling system. In this case the thin outer layer is smooth and stains black with osmium indicating a high lipid content (Fig. 5B, D, and E) that would be resistant to water uptake. In contrast, the inner layer remains white in the presence of osmium, has large cells, and is likely to absorb water (Fig. 5B, D, and F). These data suggest that the inner layer swells causing an instability, snap-buckles, and flips the aril. The energy from the flip is transferred to the seed, which is then propelled away from the parent plant. Details of this process are shown in stills showing frames at 1/5000 s intervals (Fig. 6). We propose that the aril is designed like an upside down “popper,” a hemisphere, which when turned inside out and placed on a table top, will suddenly evert, popping off the table (Supplementary Video S7a). The upside down “popper” can model seed dispersal in *Oxalis*. The cup of the upside down “popper” representing the aril holds a white cap representing the seed. When the “popper” everts, the seed is jettisoned and the “popper” falls to the side (Supplementary Video S7b).

#### Water gain builds stored elastic energy in bunchberry dogwood flowers.

Bunchberry flowers (*C. canadensis*) open explosively, launching their pollen into the air less than a

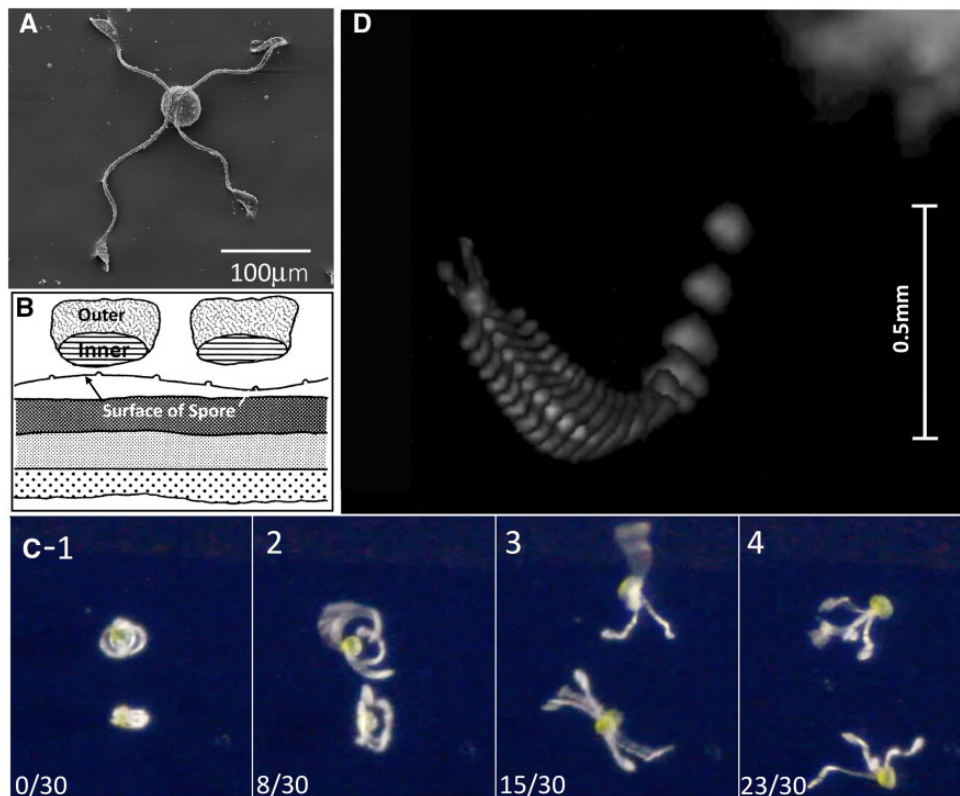


**Fig. 4** The movement of *Equisetum arvense* spores is powered by changes in the water content of elaters. (A) Electron micrograph of a single *E. arvense* spore. The two elaters are fastened to the spore slightly off-center creating four “arms.” (B) Cross section of two elaters showing the bilayers. The outer layer (gray and white) absorbs water easily causing the elaters to curl around the spore when wet. The inner layer (lined) is resistant to water uptake. The elaters are shown in relation to the spore surface and its underlying layers. Figure 4B adapted from Uehara and Kurita (1989). (C) Four stills from a video filmed at 30 fps (the numbers indicate the time frame in 30ths of seconds). Moist conditions cause the elaters to wrap around the spores (C-1). As the elaters dry, they flip out (C-2 and 3) moving the green spores to a new location. The blur is the movement in 1/30th of a second. The full video is [Supplementary Video S4](#). (D) Successive stills from a 1,000 fps video superimposed to show the unfurling of the elaters on a spore as it drops from the sporangium on the cone. When the elaters dry and unfurl the trajectory switches to upward. The full video is shown in [Supplementary Video S5](#).

millisecond after the petals begin to move, making this one of the most rapid plant movements ever recorded (Fig. 7A, B and [Supplementary Video S8](#)). Propulsion of pollen from the anther is accentuated by the presence of a thin hinge between the filament, which acts as the throwing arm, and the anther, which carries the pollen. The narrowness and flexibility of this hinge region resemble the strap on the end of a trebuchet, an instrument first designed by the Chinese and then used in medieval times for hurling boulders into an enemy’s castle (Edwards et al. 2005; Whitaker et al. 2007).

We report the data that show how water drives the explosive opening of *C. canadensis* flowers by creating stored elastic energy using turgor pressure in the stamens and petals (Edwards et al. 2005). Dehydrating flowers in sucrose solutions diminished the explosive opening of the flowers. The greater the

sucrose concentration, the less the petals reflexed and the less the anthers separated (Fig. 7C). Petals from flowers dehydrated in 2M sucrose did not reflex even when forced open; nevertheless, transferring these flowers to water overnight, a treatment that presumably restored turgor pressure, led them once again to reflex fully (35 out of 36 petals).

The floral trebuchet, although powered by turgor pressure, requires the morphology of the flower to be modified to make the stamens propulsive. We argue that the hinge is created, in part, by softening relevant parts of the structure by means of de-esterifying pectin. Where the filament attaches to the anther, a hinge forms, creating a narrow strap of tissue connecting the filament to the anther sac. The hinge, and adjacent cells in the anther from which the hinge appears to have separated, were stained bright magenta by ruthenium red (Fig. 7D, E). Insofar as

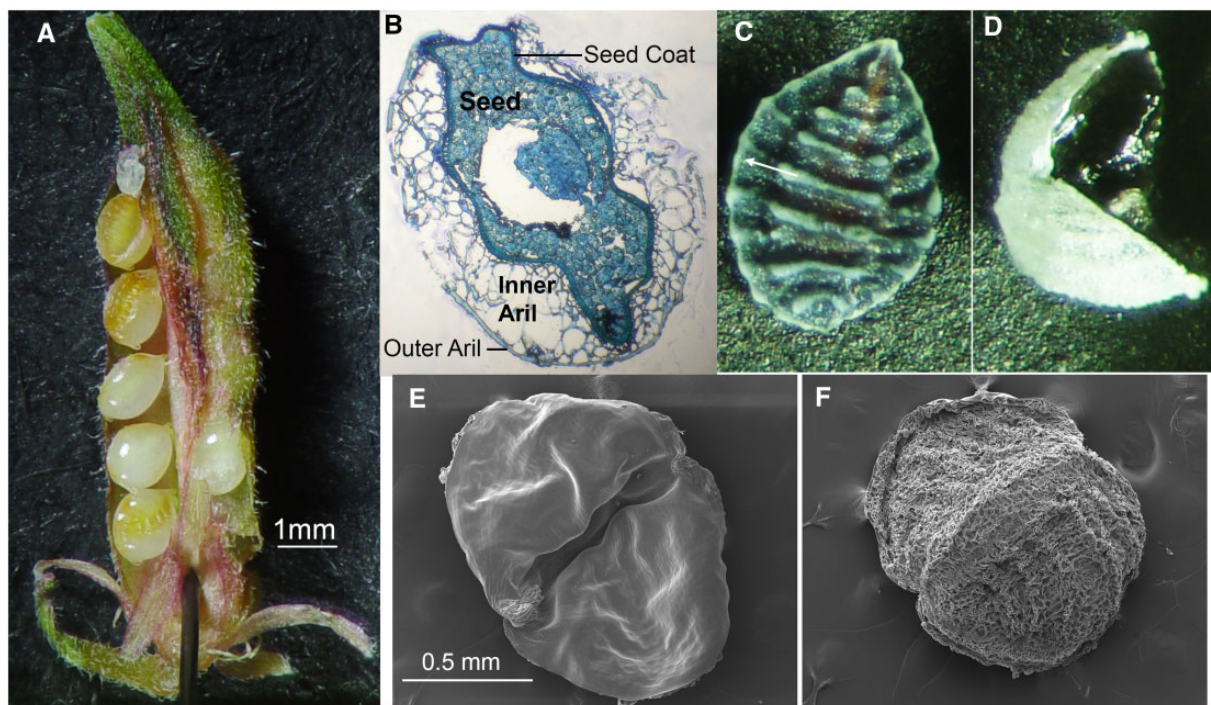


**Fig. 5** The propulsion of seeds from *Oxalis corniculata* capsules is powered by the rapid eversion of the bilayered aril. (A) Immature capsule of *O. corniculata* showing aril covered seeds aligned in a row and attached at one end. (B) Cross section of an aril covered seed showing the aril bilayer with a thin outer layer and a broad spongy inner layer. (C) *O. corniculata* seed with central ridges that line up with the initial launch direction (arrow). (D) Everted aril with the spongy inner layer (white) and the black outer layer, which has stained black with osmium. (E, F) Scanning electron micrographs of the smooth outer layer (E) and the large celled inner layer (F) of the aril photographed after it has launched the seed.

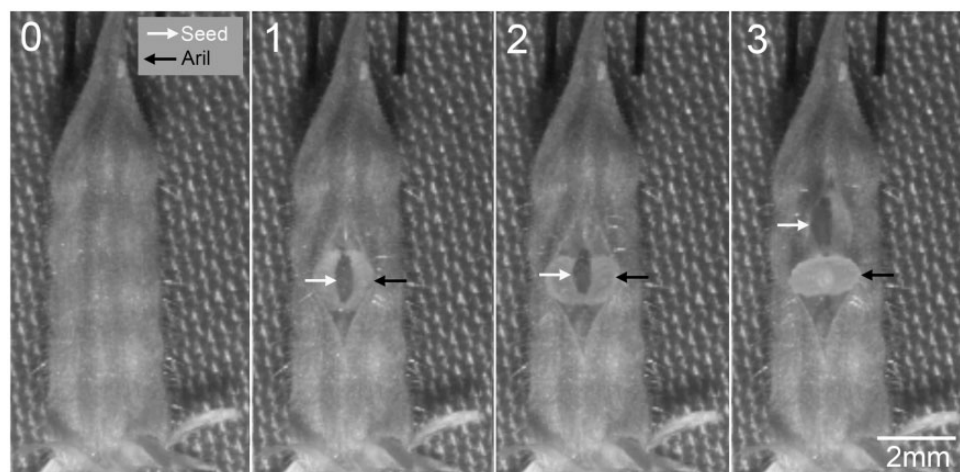


**Fig. 6** The launching of an *Oxalis corniculata* seed filmed at 50,000 fps shows the dark seed (indicated with a white arrow) is propelled by the eversion of the white aril (indicated with a black arrow). The numbers are times in 1/5000th s: 0. Closed capsule. 1. The seed is visible pocketed in the splitting aril. 2. The aril is turning inside out and the aril seed unit is pivoting upward. 3. The aril has flipped inside out propelling the seed. In the last frame the aril is fully everted so the view is of the inside of the aril.

this compound was used classically to localize acidic pectin (Sterling 1970; Luft 1971), we hypothesize that much of the pectin in the hinge and surrounding tissue has lost its esters. Supporting this hypothesis, the hinge region stains weakly if at all with

hydroxylamine hydrochloride–ferric chloride (Fig. 7F), a stain thought to preferentially bind esterified pectin (Reeve 1959). Together, these data indicate that cell walls in the hinge differ from those elsewhere in the stamen in having more acidic

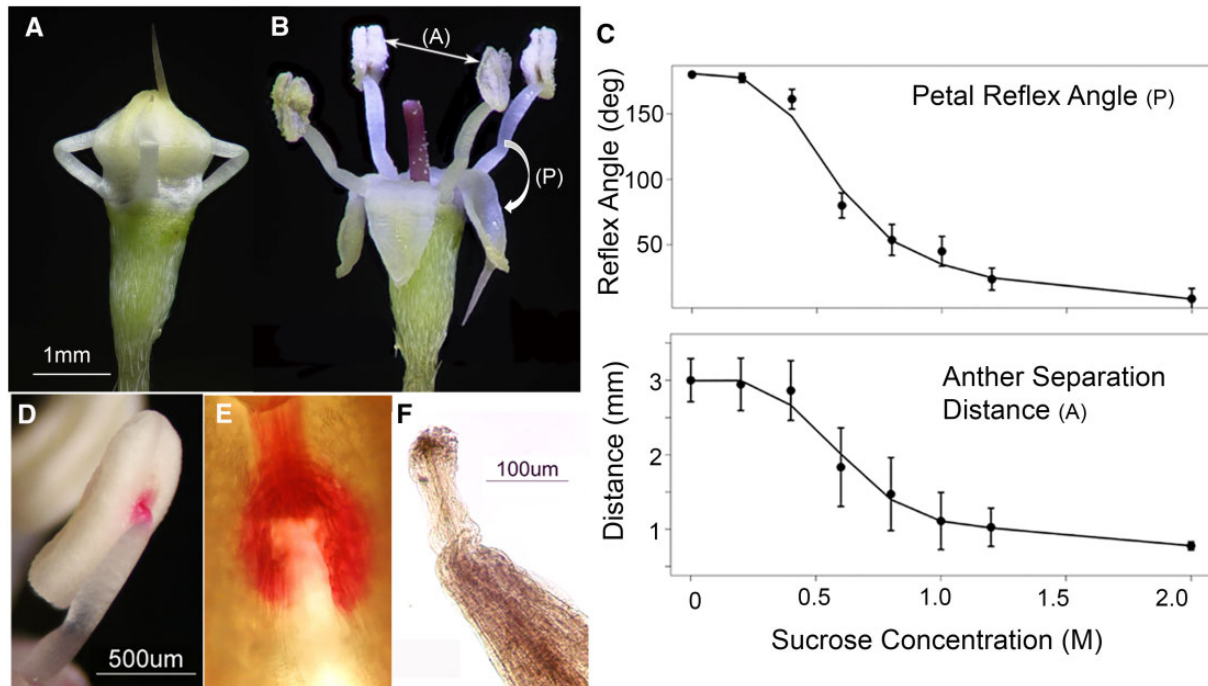


**Fig. 7** (A) Mature bunchberry dogwood flower bud. Stamen filaments protrude between the four petals, which are attached at the tip. A trigger extends from one of the petals. The trigger acts like a lever arm and when hit by a visiting insect of sufficient weight causes the petals to separate initiating floral explosion. (B) Open flower: Petals have snapped back 180°. Once released from the overlying petals (“latch”), the filaments fully extend and move apart. The double-headed arrow indicates the distance measured for anther separation (A); the curved arrow indicates the angle measured for petal reflex (P). (C) The angle that petals ( $n=36$ ) bend from vertical ( $0^\circ$ ) and the distance between opposing anthers ( $n=9$ ) for opened flowers as a function of sucrose concentration. The curve is a Loess regression fit. Data are means  $\pm$  95% confidence intervals. (D) Incubation in ruthenium red highlights the hinge region between the filament and the back of an anther. (E) Close-up of the junction between filament and anther after ruthenium red staining. (F) Hydroxylamine hydrochloride-ferric chloride staining reveals an inverse pattern; the hinge is not stained while the point of contact with the anther at the top is stained. Figures A and B are modified from Whitaker et al. (2007).

pectin, a condition that plausibly softens the tissue and is sometimes reported to precede cell separation (Daher and Braybrook 2015). These data illustrate a role for pectin in governing mechanical properties directly at the level of tissue strength.

## Summary

These five vignettes of rapid movements in plants combine an understanding of the role of water in powering rapid movements with documentation of basic morphological and physiological features, which allow the rapid movements. Together, these examples demonstrate some of the diversity of mechanisms plants use to disperse their reproductive propagules explosively.

## Acknowledgments

We thank Jeffrey Olberding, Michael Rosario, and Stephen Deban for organizing and spearheading the symposium “Playing with power: mechanisms of energy flow in organismal movement” at the 2019 meetings of the Society for Integrative and Comparative Biology.

We thank Nancy Piatczyc for overseeing the sample preparation and SEM imaging; David C. Smith for the statistical analyses and graphics in Fig. 7C; Mika Hirai for assistance in editing videos; Reiko Yamada for translating an article from the Japanese; and Ann Kremers for drawing Fig. 3E. We thank the many Williams students who helped film fast plants including Alejandro Acosta, Evelyn Tran, and Clara Hard.

## Funding

This work was supported by Williams College Research Funds and a National Science Foundation (NSF) Major Research Instrumentation award 0722532 to Williams College

## Supplementary Data

The following supplementary data are available at ICB online.

**Supplementary Video 1:** (Video1Marchantia4.mp4). Water droplet dispersal of gemmae from the splash cups of *Marchantia polymorpha* filmed at 3,000 fps.



The Video is paused briefly with arrows pointing to gemmae carried in the water droplets.

**Supplementary Video 2: (Video2Sphagnum4.mov)** Sphagnum moss capsule explosion filmed at 10,000 fps and played back at 15 fps. Credits: Joan Edwards, Clara Hard, and Dwight Whitaker.

**Supplementary Video 3: (Video3Sphagnum3MinInt.mp4)** Time-lapse video of a *Sphagnum affine* capsule explosion filmed at 3 min intervals. The successive frames correspond to the outlines shown in figure 3E. The capsule compresses and explodes in 21 min.

**Supplementary Video 4: (Video4EquisetumWalkingSpores.mp4)** Real time video of *Equisetum arvense* spores shows the curling of the elaters when wet and the sudden extension of elaters when dry. The alternate wetting and drying of the elaters effect a “walking” movement. Stills from this video are shown in 4C. Credits: Benjamin DeMeo and Joan Edwards

**Supplementary Video 5: (Video5EquisetumSporeFalling.mp4)** High-speed video of *E. arvense* spores falling from a cone filmed at 1,000 fps. The elaters are curled when the spores leave the cone and as they dry, the elaters extend. This extension corresponds to an upward movement of the spores allowing them to glide to new locations. Stills from this video were superimposed to create Figure 4D. Credit: Benjamin DeMeo and Joan Edwards

**Supplementary Video 6: (Video6Oxalis71Short.mp4)** Oxalis seed dispersal filmed at 11,001 fps and played back at 15 fps shows a seed jettisoned up to the left and the white aril dropping down. Credit: Joan Edwards and Evelyn Tran.

**Supplementary Video 7a: (Video7aPopperSloMoShort.mp4)** Slow motion video of a “popper” filmed on “Slo-mo” with an iPhone 8 at 120 fps and played back at 30 fps. Credits: Heather Williams and Joan Edwards

**Supplementary Video 7b: (Video7bUpsideDownPopperClip.mov)** Model of “popper” propelled seed. In this slow-motion video the upside-down “popper” corresponds to the aril and the white cap inside corresponds to the seed. The energy from the eversion of the popper is transferred to the cap (seed), which is jettisoned. The “popper” falls to the side. Filmed on “Slo-mo” with an iPhone 8 at 120 fps and played back at 30 fps. Credit: Heather Williams and Joan Edwards

**Supplementary Video 8: (Video8Trial55CornusExplodingFlower.mov)** Exploding bunchberry

dogwood flower. Filmed at 10,000 fps, played back at 15 fps. Note the petals flip back releasing the stamens, which propel pollen. The anthers are attached to the filament by a flexible hinge. Credit: Joan Edwards, Marta Laskowski, Dwight Whitaker and Alejandro Acosta.

## References

- Brodie HJ. 1951. The splash-cup dispersal mechanism in plants. *Can J Bot* 29:224–34.
- Daher FB, Braybrook SA. 2015. How to let go: pectin and plant cell adhesion. *Front Plant Sci* 6:523.
- Dumais J, Forterre Y. 2012. “Vegetable Dynamicks”: the role of water in plant movements. *Annu Rev Fluid Mech* 44:453–78.
- Edwards J, Whitaker D, Klionsky S, Laskowski MJ. 2005. Botany: a record-breaking pollen catapult. *Nature* 435:164.
- Equihua C. 1987. Diseminacion de yemas en *Marchantia polymorpha* L. (Hepaticae) Cryptogamie. *Bryol Lichénol* 8:199–217.
- Forterre Y. 2013. Slow, fast and furious: understanding the physics of plant movements. *J Exp Bot* 64:4745–60.
- Guigon R, Chaillout J, Jager T, Despesse G. 2008a. Harvesting raindrop energy: theory. *Smart Mater Struct* 17:015038.
- Guigon R, Chaillout J, Jager T, Despesse G. 2008b. Harvesting raindrop energy: experimental study. *Smart Mater Struct* 17:015039.
- Harris N, Spence J, Oparaka KJ. 1994. General and enzyme histochemistry. In: Harris N, Oparaka KJ, editors. *Plant cell biology: a practical approach*. Oxford: IRL Press at Oxford University Press. p. 51–68.
- Ilyas MA, Swingler J. 2017. Towards a prototype module for piezoelectric energy harvesting from raindrop impacts. *Energy* 125:716–25.
- Lenton TM, Crouch M, Johnson M, Pires N, Dolan L. 2012. First plants cooled the Ordovician. *Nat Geosci* 5:86–9.
- Lovett Doust L, MacKinnon A, Lovett Doust J. 1985. Biology of Canadian weeds. 71. *Oxalis stricta* L., *O. corniculata* L., *O. dillenii* Jacq. spp. *dillenii* and *O. dillenii* Jacq. ssp. *filipes* (Small) Eiten. *Can J Plant Sci* 65:691–709.
- Luft JH. 1971. Ruthenium red and violet. I. Chemistry, purification, methods of use for electron microscopy and mechanism of action. *Anat Rec* 171:347–68.
- Marmottant P, Ponomarenko A, Bienaimé D. 2013. The walk and jump of *Equisetum* spores. *Proc R Soc B* 280:20131465.
- Nakanishi H. 2002. Splash seed dispersal by raindrops. *Ecol Res* 17:663–71.
- Newcombe FC. 1888. Spore-dissemination of *Equisetum*. *Bot Gaz* 13:173–8.
- Perera KCR, Sampath BG, Dassanayake VPC, Hapuwatte BM. 2014. Harvesting of kinetic energy of the raindrops. *Int Scholar Sci Res Innov* 8:325–30.
- Qiu Y. 2008. Phylogeny and evolution of charophytic algae and land plants. *J Syst Evol* 46:287–306.
- Qiu YL, Cho Y, Cox JC, Palmer JD. 1998. The gain of three mitochondrial introns identifies liverworts as the earliest land plants. *Nature* 394:671–4.

- R Core Team. 2017. R: a language and environment for statistical computing. Vienna, Austria: R Foundation for Statistical Computing (<http://www.R-project.org/>).
- Reeve RM. 1959. A specific hydroxylamine-ferric chloride reaction for histochemical localization of pectin. *Stain Technol* 34:209–11.
- RStudio Team. 2017. RStudio: integrated development for R. Boston (MA): RStudio, Inc. (<http://www.rstudio.com/>).
- Sterling C. 1970. Crystal-structure of ruthenium red and stereochemistry of its pectic stain. *Am J Bot* 57:172–5.
- Uehara K, Kurita S. 1989. An ultrastructural study of spore wall morphogenesis in *Equisetum arvense*. *Am J Bot* 76:939–51.
- Ueno J. 1975. Movemng (sic) mechanism of elaters in the spore of *Equisetum arvense*. *Jpn J Palynol* 15:67–71.
- Villarreal AJC, Crandall-Stotler BJ, Hart ML, Long DG, Forrest LL. 2016. Divergence times and the evolution of morphological complexity in an early land plant lineage (Marchantiopsida) with a slow molecular rate. *New Phytol* 209:1734–46.
- Whitaker DL, Edwards J. 2010. *Sphagnum* moss disperses spores with vortex rings. *Science* 329:406.
- Whitaker DL, Webster LA, Edwards J. 2007. The biomechanics of *Cornus canadensis* stamens are ideal for catapulting pollen vertically. *Funct Ecol* 21:219–25.
- Yeats TH, Rose JKC. 2013. The formation and function of plant cuticles. *Plant Physiol* 163:5–20.